A new family of sp^3-hybridized carbon phases*

Ning Xu(徐宁)[1,†], Jian-Fu Li(李建福)[2], Bo-Long Huang(黄勃龙)[2], and Bao-Lin Wang(王保林)[1]

[1] *Department of Physics, Yancheng Institute of Technology, Yancheng* 224051, *China*
[2] *Department of Physics and Materials Science, City University of Hong Kong, Hong Kong, China*

(Received 24 April 2015; revised manuscript received 6 September 2015; published online 8 December 2015)

A new family of superhard carbon allotropes C48($2i+1$) is constructed by alternating even 4 and 8 membered rings. These new carbon allotropes are of a spatially antisymmetrical structure, compared with the symmetrical structures of *bct*-C4, *Z*-carbon, and *P*-carbon. Our calculations show that bulk moduli of C48($2i+1$) are larger than that of *c*-BN and smaller than that of cubic-diamond. C48($2i+1$) are transparent superhard materials possessing large Vicker hardness comparable to diamond. This work can help us understand the structural phase transformations of cold-compression graphite and carbon nanotubes.

Keywords: low-temperature phase transformation, superhard carbon phase

PACS: 61.66.Bi, 61.50.Ks, 62.50.–p, 78.30.Am **DOI:** 10.1088/1674-1056/25/1/016103

1. Introduction

Superhard materials play an important role in fundamental science and technological applications, and thus they have been widely used in numerous industrial fields, such as cutting, drilling tools, polishing, and coatings for surface protecting.[1,2] Among them, diamond is the hardest known material because of the nature of their strong sp^3-hybridized covalent bonding, and has been used to fulfill most of the above mentioned industrial needs. Most of the natural diamonds are formed by carbon-containing minerals under the conditions of high temperature and pressure in the Earth's mantle. Therefore, amorphous carbon, graphite, fullerene, and carbon nanotubes (CNTs) are considered as the potential precursors to synthesize diamond-like materials in high pressure experiment. For example, graphite can be converted into the hexagonal (or cubic) diamond at pressures above 15 GPa and high temperature (1600–2500 K).[3] In contrast, cold compression of graphite,[4–14] single-walled and multi-walled CNTs[15–21] result in superhard carbon allotropes, which exhibit superior mechanical performance with the ability to indent single-crystal diamond[9,15] and differ from the crystal structure of hexagonal and cubic diamond. Consequently, several hypothetical structures are proposed to shed light on the superhard mechanism.[22–30] The experimental crystal structures of cold-compressed phases of CNTs and graphite are currently still under debate. Therefore, it is essential to examine its intrinsic structure to understand the unexpectedly high indentation hardness of the cold-compressed phases of CNTs and graphite.

When we pay more attention to the previously proposed allotropes, the *bct*-C4 phase and *Z*-carbon interest is due to its unique structure.[25–28] Interestingly, all of them can be constructed through sliding and buckling of the graphene sheets. Meanwhile, the *bct*-C4 phase can be observed at the interface of *Z*-carbon. The crystal structure of *bct*-C4 is shown in Fig. 1(a), indicating the simplest 4+8 rings pattern along the armchair orientation (direct face-to-face opposed connection of two armchair chains). Similarly, a new carbon allotrope C48 is constructed as shown in Fig. 1(b). The new C48 allotrope is different from *bct*-C4, although it has $4+8$ rings. Considering all possible even rings of carbon ($4+8$ membered rings in C48, six-membered rings in hexagonal diamond), many additional possible combinations (shown in Figs. 2(a) and 2(b)) could be expected. Therefore, it is very interesting to seek a general scheme to understand the principles of the structural formation of possible alternative superhard allotropes related to cold-compressed CNTs and graphite.

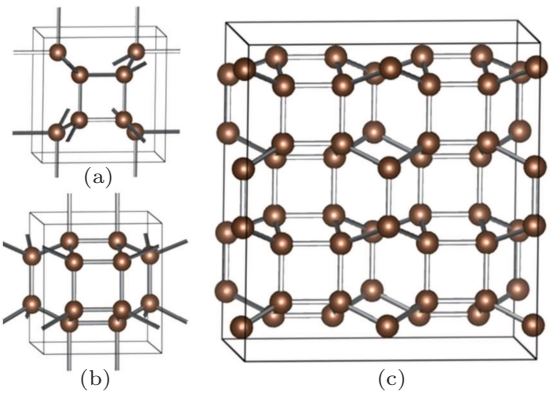


Fig. 1. (color online) (a), (b) Crystallo-graphic structures of the *bct*-C4 and the proposed C48 carbon, and (c) 2×2×1 supercell structure of C48 phase.

*Project supported by the National Natural Science Foundation of China (Grant Nos. 11174242, 11204265, 11404278, 11147007, and 11274151), the Natural Science Foundation of Jiangsu Province, China (Grant No. BK2012248), and the Scientific Research Foundation of Yancheng Institute of Technology, China (Grant No. KJC2014024).

†Corresponding author. E-mail: nxu@ycit.cn

© 2016 Chinese Physical Society and IOP Publishing Ltd

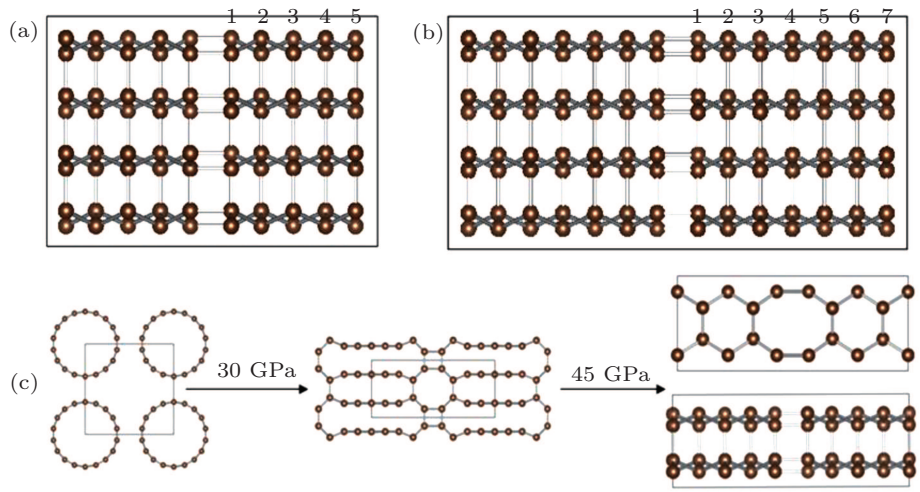


Fig. 2. (color online) (a), (b) 2D projections of the 2×2×1 suppercell of C48(5) and C48(7), and (c) high-pressure phase transition of (9,0) CNTs under different compressions.

In the present work, we report on a new family of sp^3-hybridized carbon allotropes by discussing the topological stacking of carbon atomic chains consisting of even 4 and 8 membered ring patterns. From Fig. 2, we find that the C48($2i+1$) carbon allotropes can be constructed by connecting malposed hexagonal to hexagonal diamond along the z axis. These new phases are labelled by C48($2i+1$) ($i = 1, 2, \ldots$). $2i+1$ respresents the number of layers of atoms. The conventional unit cell for C48($2i+1$) carbon has $4i$ atoms. The structures of these new phases differ from those of M-carbon, Z-carbon, W-carbon, P-carbon, S-carbon, R-carbon, and X-carbon.[31] In Fig. 2(c), we show a possible transition pathway from (9, 0) carbon nanotube to C48(5). We find that (9, 0) CNT retains its tubular structure in a pressure range from 0 to 30 GPa. The pressure-induced structure transition takes place at a pressure of 32 GPa, in which (9, 0) CNT collapse. When pressure is above 45 GPa, C48(5) can be obtained.

2. Method of calculation

The calculations were carried out by using density functional theory as implemented in the Vienna *ab initio* simulaiton package (VASP)[32] with the projector augmented-wave method employed to describe the interaction between the nucleus and valence electrons. The general gradient approximation (GGA) of the Perdew Burke Ernzerhof (PBE) parameterization[33] was adopted to describe the exchange and correlation function. A plane-wave basis set with a cutoff energy of 700 eV was used and Monkhorst–Pack[34] k meshes were chosen to ensure that all the enthalpy calculations are well converged to better than 1 meV/atom. Forces on the ions were calculated through the Hellmann–Feynman theorem allowing a full geometry optimization.

Regarding the new structural models we explored, the precisions of the electronic structures we forecast are mainly determined by both the accuracy of the lattice optimization and the corresponding Thomas–Fermi screening length averaging scheme that is for sX-LDA calculations. In the CASTEP code, the Thomas–Fermi screening length (k_{TF}) of sX-LDA was determined by evaluating the dynamical average charge density within our newly predicted structures.[35] We took this feature to accomplish the prediction of the electronic structures of the newly determined structures. This is currently unavailable in VASP but we still rely on VASP-predicted geometry structures due to their perfect balance between efficiency and accuracy. Phonon calculations have been carried out by using a supercell approach as implemented in the PHONOPY code. The XRD patterns for various structures were performed by the Materials Studio package.

3. Results and discussion

In order to investigate the relative stabilities of C48($2i+1$) phases, the calculated enthalpy difference at zero temperature with respect to graphite for different allotropes are

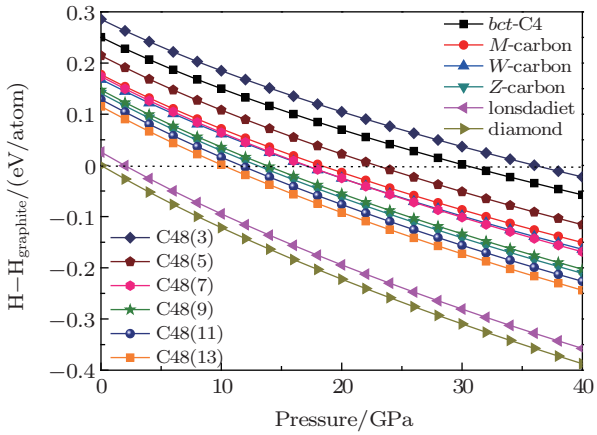


Fig. 3. (color online) Plots of calculated enthalpy difference per atom with respect to graphite versus pressure for a series of carbon allotropes. Graphite is denoted with the horizontal line at zero. The stable pressures of these proposed allotropes compared with that of graphite are labeled.

compared in Fig. 3 as a function of pressure. It is shown that the C48($2i+1$) structures with $i > 4$ are more stable than the *bct*-C4, *M*-carbon, *W*-carbon, and *Z*-carbon. Only *bct*-C4 has (almost) the largest enthalpy. C48(3) is the less stable structure than the others, and C48(5) is only more stable than *bct*-C4. The enthalpy value per atom of the C48($2i+1$) phase tends to be the value of hexagonal diamond with the increase of i.

Based on the sX-LDA method, the electronic band structure is calculated at zero pressure. $E_g = 5.476$ eV and $E_g = 6.11$ eV are obtained respectively for cubic and hexagonal diamond, which match well with the experimental results.[36] It is shown that the C48(3) carbon is a wide gap insulator with energy gap $E_g = 5.647$ eV, which is higher than that of cubic diamond and samller than that of hexagonal diamond. Analyses of electron localization functions (ELFs) (see Fig. 4(b)) and charge density difference (see Fig. 4(c)) suggest that C48(3) carbon is sp^3-hydriddized. The electron density between atoms increases with increasing pressure. These results show that the C48(3) carbon is a transparent material. Smilar properties are observed in the other C48($2i+1$) carbon phases as shown in Table 1. The C48(5) carbon has the smallest band gap $E_g = 4.743$. The band gap for C48($2i+1$) phases increases with i and tends to be the value of hexagonal diamond $E_g = 6.11$ eV.

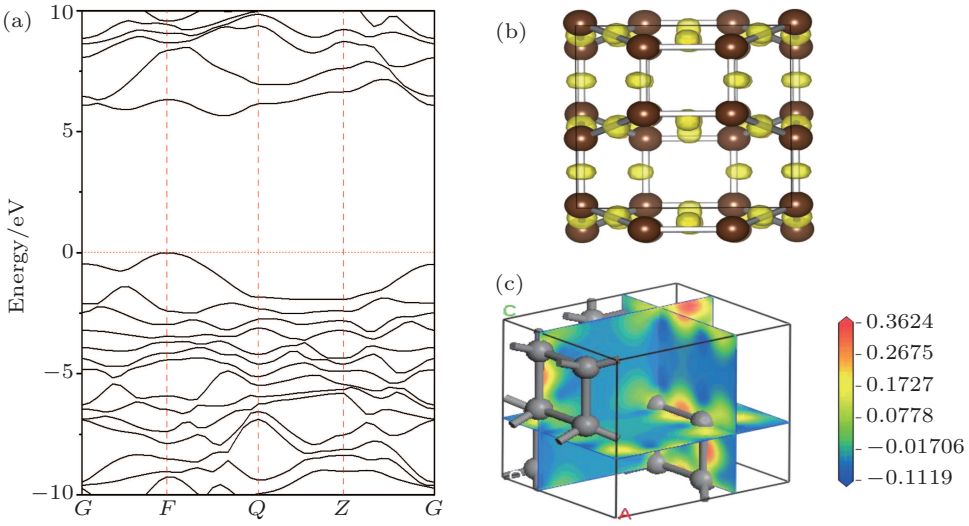


Fig. 4. (color online) (a) Calculated electronic band structure at zero pressure; (b) calculated ELF isosurface at ELF = 0.9; and (c) charge density difference for C48(3).

Table 1. Space group, lattice parameters (LP), densities (D: g·cm^{-3}), band gaps (E_g: eV), bulk moduli (B_0: GPa), shear moduli (G: GPa), Young's moduli (Y: GPa), Poisson's ratios (ν), and Vicker's hardness for *bct*-C4, *M*-Carbon, *W*-Carbon, *Z*-Carbon, Lonsdadiet, diamond, and C48.

Systems	Space group	LP/Å	D	E_g	B_0	G	Y	ν	H_v
bct-C4	$I4/mmm$	$a=b=4.3303$, $c=3.533$	3.42	3.194, 2.58,[27] 2.56[28]	430, 433.7,[27] 428.7[28]	443	989	0.1171	44.50821584
M-carbon	$C2/m$	$a=9.086$, $b=2.497$, $c=4.105$	3.45	4.842, 3.56,[27] 3.60[22]	432, 438.7,[27] 431.2[22]	476	1044	0.0975	67.8346733
W-carbon	$Pnma$	$a=9.086$, $b=2.497$, $c=4.105$	3.46	6.287, 4.39[27]	431, 444.5[27]	474	1041	0.0978	88.24206743
Z-carbon	$Cmmm$	$a=8.671$, $b=4.208$, $c=2.487$	3.52	4.024	445	494	1081	0.0950	57.07551942
Lonsdadiet	$P6_3/mmc$	$a=b=2.485$, $c=4.138$	3.60	6.110	465	551	1185	0.0750	88.11840862
Diamond	$Fd\bar{3}m$	$a=b=c=3.533$	3.64, 3.63[31]	5.68, 4.20,[27] 5.47[35]	465, 446.3[27]	546	1178	0.0780	82.18331451
C48(3)	$Pmma$	$a=4.231$, $b=3.837$, $c=4.523$	3.26	5.647	388	364	831	0.1427	76.14862682
C48(5)	$Pmma$	$a=4.191$, $b=6.341$, $c=4.418$	3.40	4.743	417	431	962	0.1151	65.74917726
C48(7)	$Pmma$	$a=4.174$, $b=8.835$, $c=4.380$	3.46	5.132	430	464	1024	0.1031	71.98063694
C48(9)	$Pmma$	$a=4.166$, $b=11.323$, $c=4.360$	3.49	5.207	437	483	1058	0.0967	73.50335501

The mechanical properties, such as bulk modulus, shear modulus, Young's modulus, Poisson's ratio, and Vicker's hardness for *bct*-C4, *M*-carbon, *W*-carbon, *Z*-carbon, hexagonal diamond, cubic diamond, C48($2i+1$) are summarized in Table 1. It is shown that the calculated lattice parameters, density, bulk modulus, and shear modulus for cubic diamond match well with the experimental results.[3,36] Further studies show that the density of C48($2i+1$) carbon phases is sparser than that of cubic and hexagonal diamond, and increases with i value increasing. The similar changing trends are observed in bulk modulus, shear modulus and Young's modulus. In contrast, Poisson's ratio decreases with the i value increasing. There are many empirical formula to simulate the Vicker's hardness.[37,38] In the present work, Vicker's hardness for these carbon alltropoes are calculated according to the method proposed by Gao *et al.*[37] We find that the C48($2i+1$)

carbon phase possesses a large Vicker hardness comparable to diamond.

The stability of a structure cannot be determined exclusively by comparing enthalpy since the structure might be subject to dynamic instabilities. Therefore, phonon dispersion curves for C48($2i+1$) are further calculated by the supercell method. In the present work, we focus on C48(3) and C48(5). C48(3) and C48(5) can be constructed by connecting malposed hexagonal to hexagonal diamond along the z axis and a grain boundary between the hexagonal diamond is observed. The primitive cell of the C48(3) phase contains 12 atoms, giving 36 phonon branches. Around the Γ point, three phonon dispersion curves are observed and no imaginary phonon frequencies are found in the whole brillouin zone (see Fig. 5(a)), indicating that the C48(3) is dynamically stable at zero pressure. Similar properties are observed in the C48(5) phase and the other C48($2i+1$) phases as shown in Fig. 5(b). The 60 phonon branches are found in Fig. 5(b), owing to 20 atoms in a unit cell of C48(5).

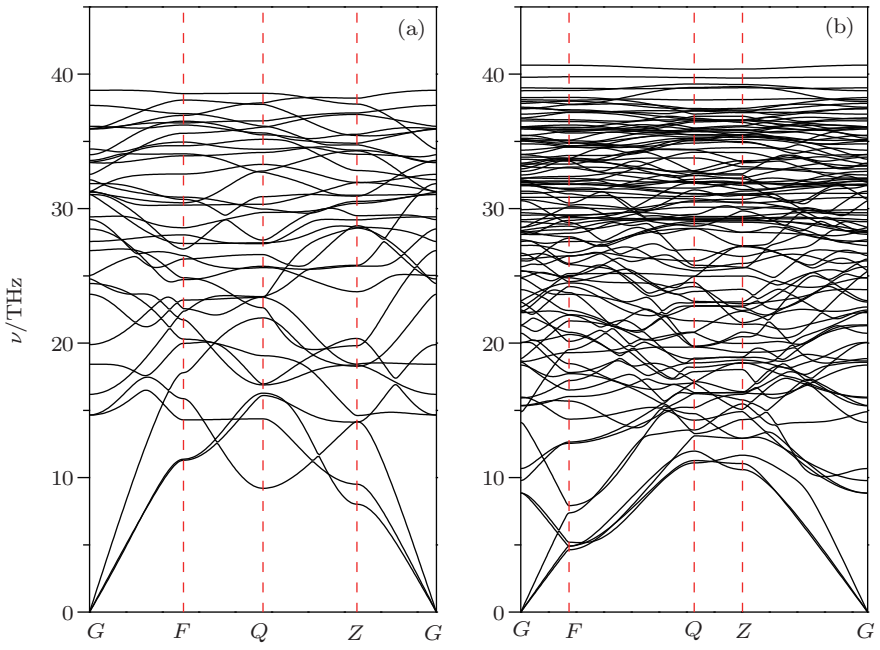


Fig. 5. (color online) Calculated phonon dispersion curves at 0 GPa for (a) C48(3) and (b) C48(5).

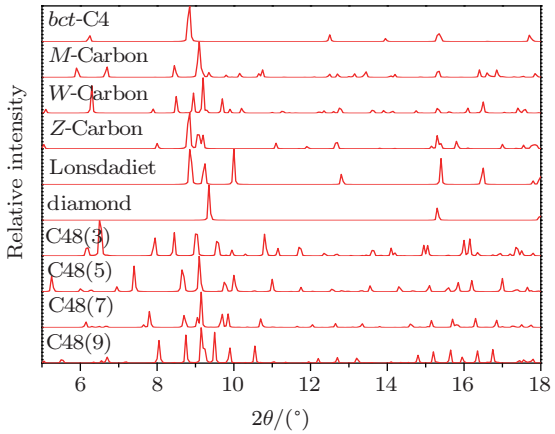


Fig. 6. (color online) Simulated XRD patterns of *bct*-C4, *M*-carbon, *W*-carbon, *Z*-carbon, hexagonal diamond, cubic diamond, and C48($2i+1$) phases (0.3329 Å radiation).

Finally, the XRD patterns of *bct*-C4, *M*-carbon, *W*-carbon, *Z*-carbon, hexagonal and cubic diamond, C48($2i+1$) phases have been simulated for instructing the experiment, by using 0.3329 Å radiation.[39] At zero pressure, the simulated intensive peak positions and relative intensities of cubic and hexagonal diamond match the experimental results very well. As is well known, each phase has its own characteristic peaks, which correspond to different crystal planes. The XRD patterns for C48($2i+1$) phases are shown in Fig. 6. Thus the nano-polycrystalline structures of C48($2i+1$) phases, constructed from carbon nanotube and graphite, can be further identified according to the additional characteristic peaks. The XRD patterns present important theoretical guidance for the experiment and can help us understand the structural phase transition of high-pressure CNTs and graphite.

4. Conclusions

In this work, we perform a comprehensive study on the lowest-enthalpy carbon phases and the phase transformation mechanisms for cold-compressed CNTs and graphite. Our calculations reveal that the phase transformation initiates and proceeds along the pathways with lowest enthalpy toward

a new family of sp^3-hybridized C48($2i+1$) phases. The cold-compressed carbon phases, constructed from CNTs and graphite, may consist of C48($2i+1$) and previously proposed *bct*-C4, *M*-carbon, *W*-carbon, *Z*-carbon, *P*-carbon, *S*-carbon, *R*-carbon, and *X*-carbon. It would be reasonable to expect that the cold-compressed phase of CNTs and graphite can be interpreted as a mixture of several of the proposed allotropes. The present results provide an excellent account for the experiment on the cold-compressed CNTs and graphite, they also provide an insight into the understanding of high-temperature phase transformation pathways for carbon structures.

References

[1] Kaner R B, Gilman J J and Tolbert S H 2005 *Science* **308** 1268
[2] Li K Y, Wang X T, Zhang F F and Xue D F 2008 *Phy. Rev. Lett.* **100** 235504
[3] Irifune T, Kurio A, Sakamoto S, Inoue T and Sumiya H 2003 *Nature* **421** 599
[4] Utsumi W and Yagi T 1991 *Science* **252** 1542
[5] Hanfland M, Syassen K and Sonnenschein R 1989 *Phys. Rev. B* **40** 1951
[6] Yagi T, Utsumi W, Yamakata M A, Kikegawa T and Shimomura O 1992 *Phys. Rev. B* **46** 6031
[7] Takano K J, Harashima H and Wakatsuki M 1991 *Jpn. J. Appl. Phys.* **30** L860
[8] Zhao Y X and Spain I L 1989 *Phys. Rev. B* **40** 993
[9] Mao W L, Mao H K, Eng P J, Trainor T P, Newville M, Kao C C, Heinz D L, Shu J, Meng Y and Hemley R J 2003 *Science* **302** 425
[10] Hanfland M, Beister H and Syassen K 1989 *Phys. Rev. B* **39** 12598
[11] Goncharov A F, Makarenko I N and Stishov S M 1989 *Sov. Phys. JETP* **69** 380
[12] Bundy F P 1967 *J. Chem. Phys.* **46** 3437
[13] Utsumi W and Yagi T 1991 *Science* **252** 1542
[14] Xu N, Li J F, Huang B L, Wang B L and Wang X L 2015 *Materials Research Express* **2** 045601
[15] Wang Z W, Zhao Y S, Tait K, Liao X Z, Schiferl D, Zha C S, Downs R T, Qian J, Zhu Y T and Shen T D 2004 *Proc. Natl. Acad. Sci.* **101** 13699
[16] Tang J, Qin L C, Sasaki T, Yudasaka M, Matsushita A and Iijima S 2000 *Phys. Rev. Lett.* **85** 1887
[17] Khabashesku V N, Gu Z N, Brinson B, Zimmerman J L and Margrave J L 2002 *J. Phys. Chem. B* **106** 11155
[18] Popov M, Kyotani M, Nemanich R J and Koga Y 2002 *Phys. Rev. B* **65** 033408
[19] Popov M, Kyotani M and Koga Y 2003 *Diam. Relat. Mater.* **12** 833
[20] Bucknum M J and Castro E A 2006 *J. Chem. Theory Comput.* **2** 775
[21] Kumar R S, Pravica M G, Cornelius A L, Nicol M F, Hu M Y and Chow P C 2007 *Diam. Relat. Mater.* **16** 1250
[22] Li Q, Ma Y M, Oganov A R, Wang H B, Wang H, Xu Y, Cui T, Mao H K and Zou G T 2009 *Phys. Rev. Lett.* **102** 175506
[23] Oganov A R and Glass C W 2006 *J. Chem. Phys.* **124** 244704
[24] Selli D, Baburin I A, Martonnak R and Leoni S 2011 *Phys. Rev. B* **84** 161411
[25] Amsler M, Flores-Livas J A, Lehtovaara L, Balima F, Ghasemi S A, Machon D, Pailhès S, Willand A, Caliste D, Botti S, San Miguel A, Goedecker S and Marques M A 2012 *Phys. Rev. Lett.* **108** 065501
[26] Zhao Z S, Xu B, Zhou X F, Wang L M, Wen B, He J L, Liu Z Y, Wang H T and Tian Y J 2011 *Phys. Rev. Lett.* **107** 215502
[27] Wang J T, Chen C F and Kawazoe Y 2011 *Phys. Rev. Lett.* **106** 075501
[28] Umemoto K, Wentzcovitch R M, Saito S and Miyake T 2010 *Phys. Rev. Lett.* **104** 125504
[29] Niu H Y, Chen X Q, Wang S B, Li D Z, Mao W L and Li Y Y 2012 *Phys. Rev. Lett.* **108** 135501
[30] Zhou R L and Zeng X C 2012 *J. Am. Chem. Soc.* **134** 7530
[31] Xu N, Li J F, Huang B L, and Wang B L and Wang X L 2015 *Mater. Res. Express* **2** 045601
[32] Kresse G and Fürthmuller J 1996 *Phys. Rev. B* **54** 11169
[33] Blochl P E 1994 *Phys. Rev. B* **50** 17953
[34] Monkhorst H J and Pack J D 1976 *Phys. Rev. B* **13** 5188
[35] Clark S J, Segall M D, Pickard C J, Hasnip P J, Probert M I J, Refson K and Payne M C 2005 *Z. Kristallogr* **220** 567
[36] Occelli F, Loubeyre P and Letoullec R 2003 *Nat. Mater.* **2** 151
[37] Gao F, He J, Wu E, Liu S, Yu D, Li D, Zhang S and Tian Y 2003 *Phys. Rev. Lett.* **91** 015502
[38] Chen X Q, Niu H Y, Li D Z and Li Y Y 2011 *Intermetallics* **19** 1275
[39] Xu N, Li J F, Huang B L, Wang B L and Wang X L 2015 *Mater. Res. Express* **2** 045601